

Pendular States and Spectra of Oriented Linear Molecules

J. M. Rost, J. C. Griffin, B. Friedrich, and D. R. Herschbach

Department of Chemistry, Harvard University, Cambridge, Massachusetts 02138

(Received 6 December 1991)

Recent experiments have demonstrated the feasibility of orienting rotationally cooled polar molecules in an electric field. The anisotropy of the Stark effect allows molecules in low rotational states to be trapped in "pendular states," confined to librate over a limited angular range about the field direction. We present calculations exhibiting the nature of these pendular states for a linear molecule and characteristic features of infrared and microwave spectra which become observable in strong fields.

PACS numbers: 33.10.-n, 33.20.Bx, 33.20.Ea, 33.55.Be

Electric-field focusing has long provided an effective means to obtain beams of oriented symmetric top molecules (or equivalent) that have a first-order Stark effect [1,2]. Such molecules in certain rotational states precess rather than tumble and hence maintain a constant projection of the dipole moment on the field direction. State selection by the focusing field thus suffices to pick out molecules with substantial orientation of the figure axis. This has enabled elegant studies of the anisotropic forces governing collisions with reactive atoms [1-4], photons [5,6], or surfaces [7]. However, the technique requires an elaborate apparatus and is not applicable when the Stark interaction is second order, as usual for diatomic, linear, or asymmetric top molecules.

A simpler technique applicable to polar molecules with either a first- or second-order Stark interaction has recently been proposed [8,9]. This exploits the extreme rotational cooling attainable in a supersonic expansion to condense a large fraction of a molecular beam into low rotational states. By sending the beam into a strong *uniform* electron field, these low- J states can be converted from pinwheeling rotors into pendular librators confined to oscillate over a limited angular range about the field direction. The pendular states are directional hybrids [10,11], comprised of linear combinations of the field-free rotor states $|J, M\rangle$ with a range of J values but the same fixed value of the M quantum number specifying the projection of the angular momentum on the field direction. For a diatomic or linear molecule with dipole moment μ and rotational constant B in a field of strength \mathcal{E} , the ratio $\omega = \mu\mathcal{E}/B$ governs the extent of hybridization of rotor states and the consequent directional localization of the pendular states.

The feasibility of this orientation technique has been demonstrated experimentally for beams of a symmetric top molecule [8,12] (methyl iodide, CH_3I) and a diatomic molecule [13,14] (iodine monochloride, ICl). The overall orientation achieved was modest, however, since in those experiments the ω values for the highest field strengths used were rather low, only 1.7 (CH_3I) and 3.7 (ICl), respectively. Block, Bohac, and Miller [15] have now provided a far more incisive demonstration of pendular orientation, by measuring infrared spectra with sub-Doppler resolution for the linear trimer of hydrogen

cyanide, $(\text{HCN})_3$. By virtue of its extremely large dipole moment and small rotational constant, for this molecule ω values up to 360 were attained. For such a high- ω value, over 100 pendular states are bound by the Stark potential, including all states with nominal $J \leq 10$. Here we present calculations evaluating the orientation of the pendular states and diagnostic spectral features.

For a rigid linear molecule in a uniform electric field the Schrödinger equation is

$$(\mathbf{J}^2 - \omega \cos\theta)|J, M; \omega\rangle = E|J, M; \omega\rangle, \quad (1)$$

with \mathbf{J}^2 the squared angular momentum operator, θ the angle between the molecular axis and the field direction, and E the energy in units of the rotational constant. The Stark eigenstates are labeled by the rotational quantum numbers pertaining to the field-free case, so $|J, M; \omega\rangle \rightarrow |J, M\rangle$ for $\omega \rightarrow 0$. In the presence of the field, M remains a good quantum number but within each J -manifold states with different values of $|M|$ have different energies. Tabulations of $E(J, M; \omega)$ extending into the high-field regime are available [16,17], but there seem to be no previous calculations examining the field-induced hybridization of J states or the corresponding drastic changes in line strengths which enrich the spectra with many transitions that would be forbidden in the absence of the field [18]. We have prepared a program which determines in addition to E the Stark eigenfunctions $|J, M; \omega\rangle$ as linear combinations of spherical harmonics, with subroutines which evaluate the expectation value of the orientation cosine, $\langle \cos\theta \rangle$, and compute spectral transitions and line strengths.

Figure 1 illustrates for $\omega = 100$ how E and $\langle \cos\theta \rangle$ vary with J and M . The Stark interaction potential is attractive for $|\theta| \leq 90^\circ$ and repulsive elsewhere. Hence, for the bound pendular states with negative energies (below the $J=0$ field-free level), the librating dipole is limited to the attractive range with $\langle \cos\theta \rangle$ positive. For the pendular states with positive energies the range of favored θ directions depends strongly on the initial "tilt angle" of \mathbf{J} in the semiclassical vector model [19], given by $\alpha = \cos^{-1}|M|/[J(J+1)]^{1/2}$. When the tilt angle is large (i.e., $J - |M|$ large or α near $\sim 90^\circ$), the plane of the rotating dipole lies close to the electric-field direction. The dipole then speeds up as it swings through the attractive

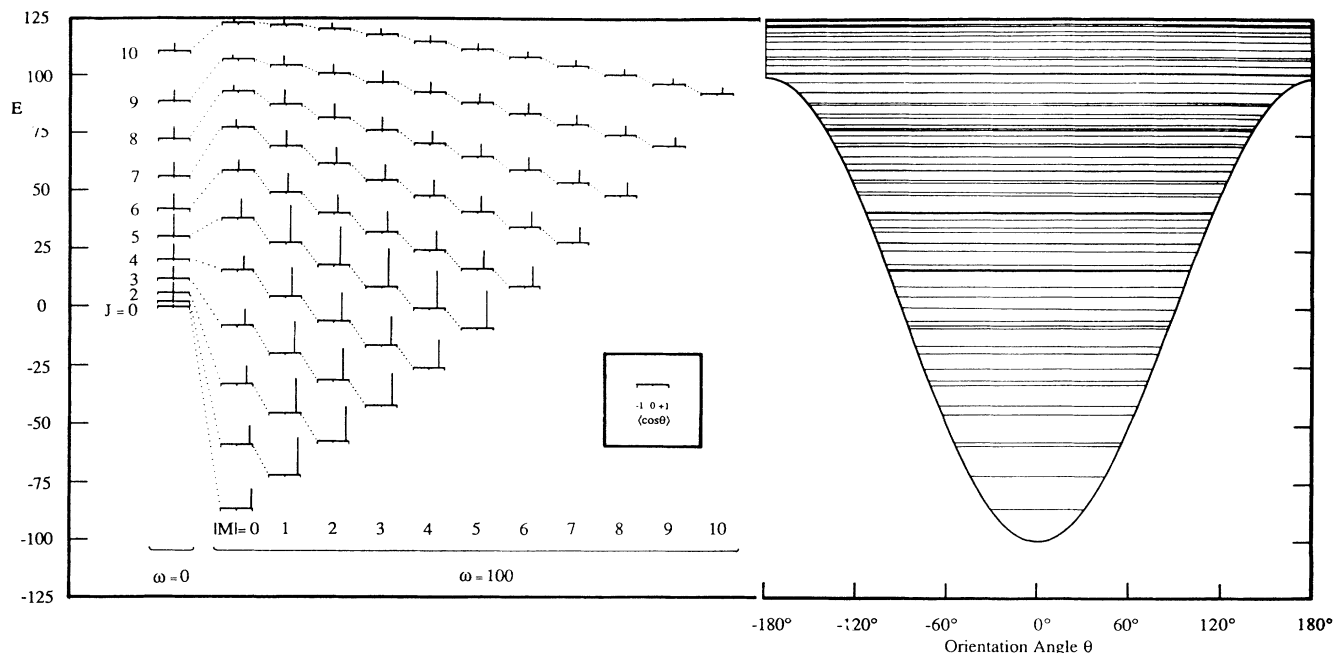


FIG. 1. Stark shifts of energy levels and orientation for a linear polar molecule. Left: field-free rotational levels ($\omega=0$; M degenerate). Middle: Stark levels sorted by $|M|$ for a high field ($\omega=100$). Right: interaction potential, $-\omega \cos\theta$, with energy levels indicated. Energies in units of rotational constant B . Position of vertical bar on each level indicates the expectation value of the orientation cosine, $\langle \cos\theta \rangle$; the height of this bar indicates thermal population (for reduced temperature $Y=65$). Bars for $\omega=0$ are reduced by a factor of 10.

range and slows down as it approaches the repulsive barrier. On average, the dipole in such states points the "wrong way," with $|\theta| \geq 90^\circ$, so it experiences net repulsion and has negative $\langle \cos\theta \rangle$ [20]. For the unbound pinwheeling states with positive energies slightly above the Stark barrier, $\langle \cos\theta \rangle$ likewise varies with the tilt angle; when averaged for these nearly degenerate states or for states substantially above the barrier, the net $\langle \cos\theta \rangle$ becomes nearly zero. To attain substantial overall orientation of a beam it is thus essential that the population distribution allows the pendular states with negative energies to outweigh the higher states.

When the molecular beam enters the electric field, the initial population p_J of each field-free rotational J manifold (degenerate in M) is adiabatically transformed into the Stark eigenstates. Within each J manifold the population of the Stark states therefore is $p_J/(2J+1)$ for $M=0$ and $2p_J/(2J+1)$ for $|M|>0$. In our program, population averages are carried out using p_J for a rotational Boltzmann distribution, which depends on a single reduced temperature variable, $Y = k_B T_{\text{rot}}/B$. Evidence for approximately Boltzmann rotational distributions in supersonic beams is abundant but imprecise [21]. Table I lists our calculated values of $\langle \cos\theta \rangle$ for the best oriented state ($J=M=0$) and the population-averaged $\langle \cos\theta \rangle$ for the three experiments [8,13,15] that have so far employed pendular orientation. Although a small rotational constant fosters good orientation of the lowest pendular states by enhancing the value of ω , it also enhances Y and

thus reduces the population of low- J states.

Figure 2 correlates the field-free rotor states with the harmonic librorator states for the $\omega \rightarrow \infty$ limit. The Stark energies for pendular states in that limit become those for a two-dimensional angular oscillator,

$$E(J, M; \omega) \rightarrow -\omega + (v_p + 1)(2\omega)^{1/2}, \quad (2)$$

where $v_p = 2n_\theta + |M| = 0, 1, 2, \dots$ is the total number of vibrational quanta, with $n_\theta = J - |M|$ the number of θ nodes (in the range $0^\circ - 180^\circ$), and $|M| = 0, 1, 2, \dots, J$ is the number of ϕ nodes (in $0^\circ - 360^\circ$). Hence, $v_p = 2J - |M|$. For spectroscopic transitions, electric dipole selection rules impose as usual $\Delta M = 0$ (for radiation polarized parallel to the static \mathcal{E} field) or $\Delta M = \pm 1$ (for perpendicular polarization), but as ω increases hybridization causes the field-free rule $\Delta J = \pm 1$ to break down. However, as seen from the correlation diagram, when ω becomes very large the spectra become simpler as levels

TABLE I. Values of $\langle \cos\theta \rangle$ for lowest state (LS) and thermal average (TA).

Molecule	μ (D)	B (cm^{-1})	T_{rot} (K)	ω	$\langle \cos\theta \rangle_{\text{LS}}$	$\langle \cos\theta \rangle_{\text{TA}}$
CH ₃ I	1.65	0.253	~ 30	1.7	0.438	0.0065
ICI	1.24	0.114	~ 15	3.7	0.625	0.0105
(HCN) ₃	10.6	0.0156	1.4	23	0.852	0.0057
				100	0.929	0.180
				360	0.963	0.372

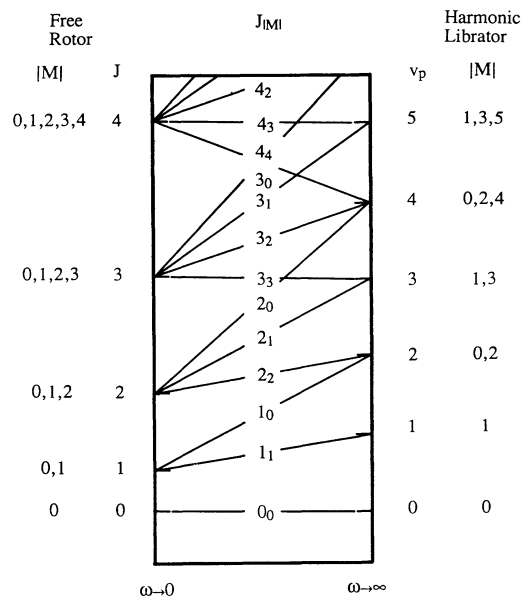


FIG. 2. Correlation diagram between field-free ($\omega=0$) rotational states $|J, M\rangle$ for a linear molecule and high-field ($\omega \rightarrow \infty$ limit) harmonic librator states $|v_p, M\rangle$ specified in Eq. (2).

with different $|M|$ but the same v_p converge. Then the parallel transitions correspond to $\Delta v_p = 2$ (so weaken as ω grows) and perpendicular transitions to $\Delta v_p = 1$ (so strengthen as ω grows). A diagnostic test for pendular orientation is to measure the perpendicular Stark spectra for large ω and thereby observe directly the pendular fundamental frequency, $\Delta E \rightarrow (2\omega)^{1/2}$.

Figure 3 presents calculated spectra for $\omega=0, 23, 100,$ and 360 corresponding to the experimental conditions of Block, Bohac, and Miller [15]. Their infrared spectra pertain to the $v_3=0 \rightarrow 1$ band of a vibrational mode of the $(\text{HCN})_3$ trimer, assigned as a symmetric combination of the two C-H stretches linked by hydrogen bonds [22]. From the field-free spectra we find the rotational temperature is 1.4 K, corresponding to $Y=65$. These spectra also exhibit distinct broadening [22] due chiefly to vibrational predissociation of the $v_3=1$ level (lifetime 2.8 ns); the total FWHM (15 MHz instrumental, 56 MHz predissociative) is 0.0024 cm^{-1} . In constructing our calculated Stark spectra, we used a Lorentzian line shape with this width. The experimental geometry pertains to perpendicular transitions, and the observed spectra [15] indeed agree closely with our calculated $\Delta M = \pm 1$ spectra. As the field strength is increased, the P and R branch structure of the vibrational bands (at $\omega=0$) first develops complicated Stark substructure in the low- J region (evident at $\omega=23$), but this collapses into two broad clumps (as seen at $\omega \geq 100$) corresponding to the $\Delta v_p = \pm 1$ pendular transitions. The shape of these clumps reflects both the anharmonicity of the $\cos\theta$ potential and the thermal population distribution. The outer regions contain the lowest- J transitions, so individual lines are

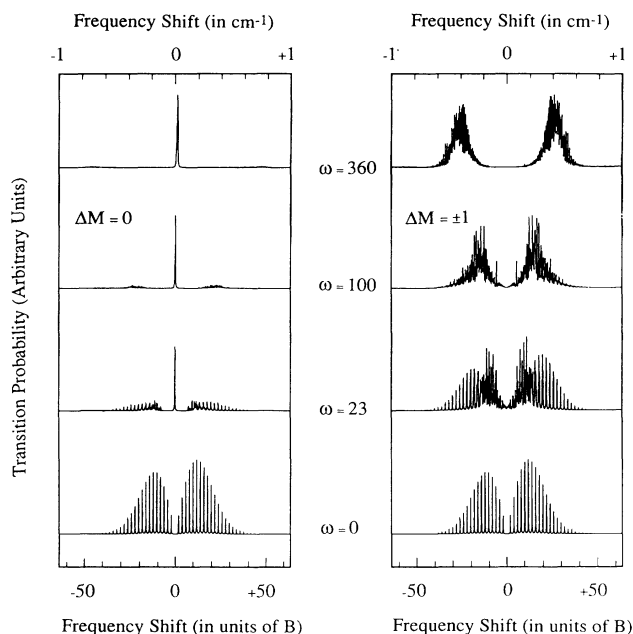


FIG. 3. Calculated vibration-rotation spectra corresponding to experimental conditions of Block, Bohac, and Miller [15], for parallel (left) and perpendicular (right) transitions. The lower abscissa scale is in units of rotational constant B ; the upper scale is in cm^{-1} relative to the band origin of the v_3 vibrational mode. Parameters: dipole moment = 10.6 Debye units; rotational constant $B = 0.015654 \text{ cm}^{-1}$ ($v_3=0$) and 0.015690 cm^{-1} ($v_3=1$); band origin $v_3 = 3212.933 \text{ cm}^{-1}$; Lorentzian FWHM = 0.0024 cm^{-1} ; rotational temperature $T_{\text{rot}} = 1.4 \text{ K}$. Reduced variables: $\omega = 0.01679 \mu(\text{D}) \mathcal{E}(\text{kV/cm}) / B(\text{cm}^{-1})$; $Y = 0.6961 T_{\text{rot}}(\text{K}) / B(\text{cm}^{-1})$.

most resolvable there, whereas the drooping inner edges exhibit the exponential decline of the Boltzmann factor. The observed median spacing between the clumps at $\omega = 360$ indicates that the typical pendular period there is about 10^{-10} s .

In contrast, $\Delta M = 0$ transitions produce a $\Delta v_p = 0$ (allowed in combination with $\Delta v_3 = 1$) and $\Delta v_p = \pm 2$ bands. The very intense $\Delta v_p = 0$ band, which exists only for oriented molecules, is in effect a Q branch to which every Stark level contributes in proportion to its value of $\langle \cos\theta \rangle$. This band is only slightly broader than the Lorentzian linewidth, since the rotational constants [22] for the $v_3=0$ and $v_3=1$ levels are very similar. The $\Delta v_p = \pm 2$ bands are much weaker, and fade away when ω becomes large enough to draw a large fraction of the populated levels down into the harmonic portion of the Stark potential. Observation of parallel transitions, particularly the very distinctive $\Delta v_p = 0$ band, thus offers another key diagnostic test for pendular orientation.

Figure 4 shows the variation with ω of line strengths for typical rotational transitions, for comparison with anticipated measurements of microwave Stark spectra for the $(\text{HCN})_3$ trimer [23]. Since in recording microwave

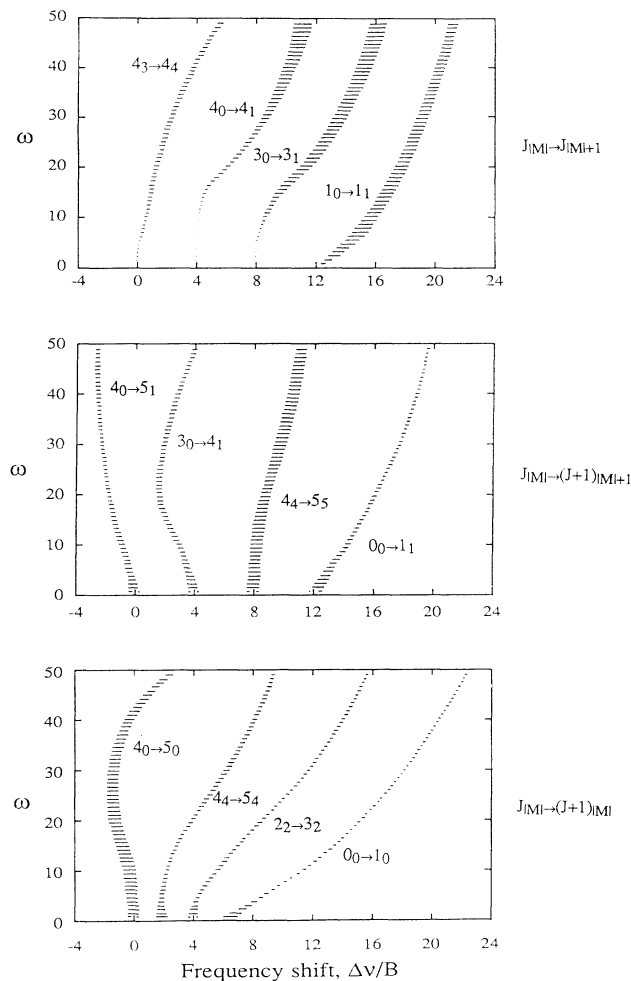


FIG. 4. Shifts from field-free values of line strengths (divided by $2J+1$) and frequencies of Stark lobes for representative rotational transitions of a linear polar molecule (without nuclear-spin hyperfine structure). For clarity, the origins for various transitions are displaced along the abscissa scale (in units of B). Lengths of horizontal bars indicate changes of line strengths; in the $J_{|M|} \rightarrow J_{|M|+1}$ panel they are magnified by a factor of 5.

spectra individual Stark lobes are followed, we show shifts from the field-free frequency and line strength. For large ω these shifts are often drastic and many transitions appear that are forbidden for field-free spectra, but hyperfine structure due to quadrupolar nuclei is simplified because the strong field uncouples the nuclear spin from molecular rotation [24,25]. Two of the illustrative panels pertain to the principal $J \rightarrow J+1$ progression. Since the low- J states become pendular most readily, as ω increases the parallel transitions shift more rapidly to higher frequency but decrease monotonically in intensity. For the perpendicular transitions, lines with maximum $|M|$ shift upwards most markedly; the intensities initially decrease but ultimately increase as the states become strongly pen-

dular. The third panel pertains to $J \rightarrow J$ perpendicular transitions, forbidden for $\omega=0$. These are a distinctive feature, only observable for oriented molecules.

We are grateful to Professor Roger Miller and his colleagues at the University of North Carolina for resonant discussions and hospitality during a visit by D.R.H. as Michael Polanyi Lecturer. Support of this work by a DAAD-NATO Fellowship for J.M.R. and a Meitec Junior Fellowship for J.C.G. is thankfully acknowledged.

- [1] R. J. Beuhler, R. B. Bernstein, and K. H. Kramer, *J. Am. Chem. Soc.* **88**, 5331 (1966).
- [2] P. R. Brooks and E. M. Jones, *J. Chem. Phys.* **45**, 3449 (1966).
- [3] P. W. Harland, H. S. Carman, L. F. Phillips, and P. R. Brooks, *J. Phys. Chem.* **95**, 8137 (1991), and work cited therein.
- [4] M. H. M. Janssen, D. H. Parker, and S. Stolte, *J. Phys. Chem.* **95**, 8142 (1991).
- [5] S. Kaesdorf, G. Schönhense, and U. Heinzmann, *Phys. Rev. Lett.* **54**, 885 (1985).
- [6] S. R. Gandhi and R. B. Bernstein, *Z. Phys. D* **10**, 179 (1988).
- [7] V. A. Cho and R. B. Bernstein, *J. Phys. Chem.* **95**, 8129 (1991), and work cited therein.
- [8] H. J. Loesch and A. Remscheid, *J. Chem. Phys.* **93**, 4779 (1990).
- [9] B. Friedrich and D. R. Herschbach, *Z. Phys. D* **18**, 153 (1991).
- [10] S. Kais and R. D. Levine, *J. Phys. Chem.* **91**, 5462 (1987).
- [11] B. Friedrich, D. P. Pullman, and D. R. Herschbach, *J. Phys. Chem.* **95**, 8118 (1991).
- [12] H. J. Loesch and A. Remscheid, *J. Phys. Chem.* **95**, 8194 (1991).
- [13] B. Friedrich and D. R. Herschbach, *Nature (London)* **353**, 412 (1991).
- [14] H. J. Loesch, as quoted by S. Borman, *Chem. Eng. News* **69** (43), 19 (1991).
- [15] P. Block, E. Bohac, and R. E. Miller, following Letter, *Phys. Rev. Lett.* **68**, 1303 (1992).
- [16] K. von Meyenn, *Z. Phys.* **231**, 154 (1970).
- [17] E. S. Krayachko and O. E. Yanovitskii, *Int. J. Quantum Chem.* **40**, 33 (1991).
- [18] Dipole matrix elements for the high-field limit are given by J. M. Rost and J. S. Briggs, *J. Phys. B* **24**, 4293 (1991).
- [19] R. N. Zare, *Angular Momentum* (Wiley-Interscience, New York, 1988), pp. 12–17.
- [20] O. Stern, as quoted by R. G. F. Fraser, *Molecular Rays* (Cambridge Univ. Press, London, 1931), pp. 156–160.
- [21] D. P. Pullman, B. Friedrich, and D. R. Herschbach, *J. Chem. Phys.* **93**, 3224 (1990), and work cited therein.
- [22] K. W. Jucks and R. E. Miller, *J. Chem. Phys.* **88**, 2196 (1988).
- [23] R. S. Ruoff, T. Emilsson, T. D. Klots, C. Chuang, and H. S. Gutowsky, *J. Chem. Phys.* **89**, 138 (1988).
- [24] U. Fano, *J. Res. Natl. Bur. Stand.* **40**, 215 (1948).
- [25] S. R. Gandhi and R. B. Bernstein, *J. Chem. Phys.* **93**, 4024 (1990).